arXiv:1408.1802v2 [astro-ph.SR] 12 Aug 2014

18th Cambridge Workshop on Cool Stars, Stellar Systems, and the Sun
Proceedings of Lowell Observatory (9-13 June 2014)
Edited by G. van Belle & H. Harris

MHD simulations of near-surface convection in cool main-sequence stars

Benjamin Beeck[1], Manfred Schüssler[1], Ansgar Reiners[2]

[1]*Max Planck Institute for Solar System Research, Justus-von-Liebig-Weg 3, 37077 Göttingen, Germany*

[2]*Institute for Astrophysics, University of Göttingen, Friedrich-Hund-Platz 1, 37077 Göttingen, Germany*

Abstract. The solar photospheric magnetic field is highly structured owing to its interaction with the convective flows. Its local structure has a strong influence on the profiles of spectral lines not only by virtue of the Zeeman effect, but also through the modification of the thermodynamical structure (e.g. line weakening in hot small-scale magnetic structures). Many stars harbor surface magnetic fields comparable to or larger than the Sun at solar maximum. Therefore, a strong influence of the field on the surface convection and on spectral line profiles can be expected.

We carried out 3D local-box MHD simulations of unipolar magnetized regions (average fields of 20, 100, and 500G) with parameters corresponding to six main-sequence stars (spectral types F3V to M2V). The influence of the magnetic field on the convection and the local thermodynamical structure were analyzed in detail. For three spectral lines, we determined the impact of the magnetic field on the disc-integrated Stokes-I profiles. Line weakening has in many cases a stronger impact on the spectral line profiles than the Zeeman effect. Moreover, for some stars, the correlation between the magnetic field and the vertical velocity strongly influences the line shapes. These effects can impair determinations of stellar magnetic fields since currently used methods neglect the local structure of the magnetic field and its interaction with the convective flows. The MHD simulations presented can be used to quantify these effects and thus help to improve magnetic field measurements of cool main-sequence stars.

1. Introduction

The interaction between magnetic fields and convective flows plays an important role in the convectively unstable outer layers of cool main-sequence stars. In the Sun, many local effects of the magnetic field (sunspots, faculae, chromospheric activity, etc.) can be observed in great detail. For other stars such spatially highly resolved observations are, however, not possible.

In recent years, many successful magnetic field detections in cool main-sequence stars exploiting the Zeeman effect have been reported (see Reiners, 2012, for a review). With Zeeman Doppler imaging (ZDI) it has become possible to extract the large-scale geometry of the magnetic field of some rapidly rotating

cool stars (see, e. g., Donati et al., 2003). However, for most measurements of stellar magnetic fields the spatial correlations between the velocity field, temperature, pressure, and density with the magnetic field have to be ignored as they are unknown. In the Sun, the magnetic field in the photosphere is concentrated in regions, which can be much brighter or much darker (i. e., cooler and denser) than the quiet Sun. It is thus likely that the magnetic field has a similar local impact on the photospheres of other stars. As the spectral line profiles which are used to determine the magnetic field are also sensitive to thermodynamic quantities (temperature, pressure, etc.), their disk-integrated profiles including the Zeeman broadening/splitting and the polarization are affected by the correlation between thermodynamic properties and the magnetic field. For example, Rosén & Kuchukhov (2012) showed that the ZDI reconstruction of the magnetic field from artificial spectroscopic data fails if the magnetic field is concentrated in dark spots.

We have run three-dimensional magnetohydrodynamic simulations in order to investigate the details of the magnetoconvection in the near surface layers of cool main-sequence stars. We analyze the impact of a moderate unipolar magnetic field (20 to 500 G horizontally averaged flux density) on the convection and on the disk-integrated profiles of three sample spectral lines.

2. MHD Simulations with MURaM

2.1 MURaM code

The MURaM code solves the fully compressible MHD equations on a three-dimensional Cartesian grid with explicit time stepping. Radiative transport is approximated with the opacity binning method (τ sorting for the individual atmospheres) with four bins resolved in three ray directions per octant(Vögler et al., 2004, and references therein). The code uses the OPAL equation of state (Rogers et al., 1996) which includes partial ionization. Opacities and equation of state used are for the solar chemical composition published by Anders & Grevesse (1989). For more details on the code, see Vögler (2003) and Vögler et al. (2005); for a comparison between MURaM and two similar codes for solar parameters see Beeck et al. (2012). The version of the code used for the simulations considered here, uses the slope limiter and the modified Lorentz force introduced by Rempel et al. (2009).

2.2 Simulation setup

We simulated the near-surface convection with the properties resembling those of six cool main-sequence stars that roughly correspond to spectral types F3V, G2V (Sun), K0V, K5V, M0V, and M2V. The sizes of the computational domain were adapted to the horizontal scale of the convection (granulation) and to the pressure scale heights (see Beeck et al., 2013a). As initial condition and as a reference non-magnetic (hydrodynamic) simulations were run. These were analyzed in detail in Beeck et al. (2013a) and Beeck et al. (2013b). For each spectral type three magnetic simulations were run. The initial condition for the magnetic field in these three runs was a vertical homogeneous field of 20, 100, and 500 G, respectively. After an initial restructuring phase lasting about 10–30 stellar minutes, the simulations reached statistically stationary states. The snapshots considered

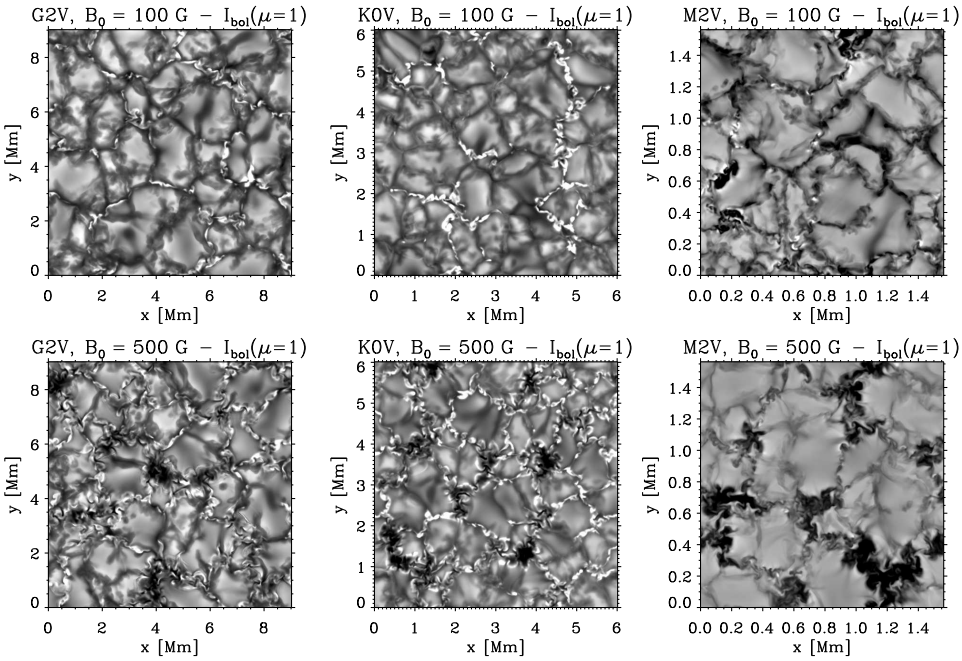

Figure 1.: *Bolometric intensity maps (at vertical view, i. e.* $\mu = \cos\theta = 1$*) for one snapshot of six of the MHD simulations. The approximate spectral types and the mean vertical magnetic field are given in the titles of each panel. The gray scale saturates at* ± 2.5 *standard deviations from the mean intensity.*

were all taken from this "relaxed" stationary phase, about 1–2 h (stellar time) after the magnetic field was introduced (for more details, see Beeck, 2014).

3. Results

3.1 Surface magnetoconvection

Figure 1 shows the vertical bolometric intensity of six of the magnetic runs (G2V, K0V, and M2V, each with 100 and 500 G average vertical magnetic field strength). The magnetic field is advected into the intergranular lanes where it accumulates and forms structures with a local field strength of roughly 1.5–2.5 kG, which are visible in the intensity images because they have either reduced or enhanced intensity. In general, smaller magnetic flux concentrations are bright and larger ones are dark. As the evacuation caused by the magnetic pressure in these structures produces depressions of the optical surface (or enhances the already existing depressions in the downflow lanes), hot side walls form around the magnetic flux concentrations. These can efficiently heat small structures (large side-wall area compared to the volume of the structure). If these depressions become much wider than they are deep, the sidewall heating is less efficient. The structures then become dark in the absence of sufficient convective heating, because magnetic flux concentrations suppress horizontal inflows owing to the strong vertical magnetic field. Figure 1 also illustrates that there is a substantial difference be-

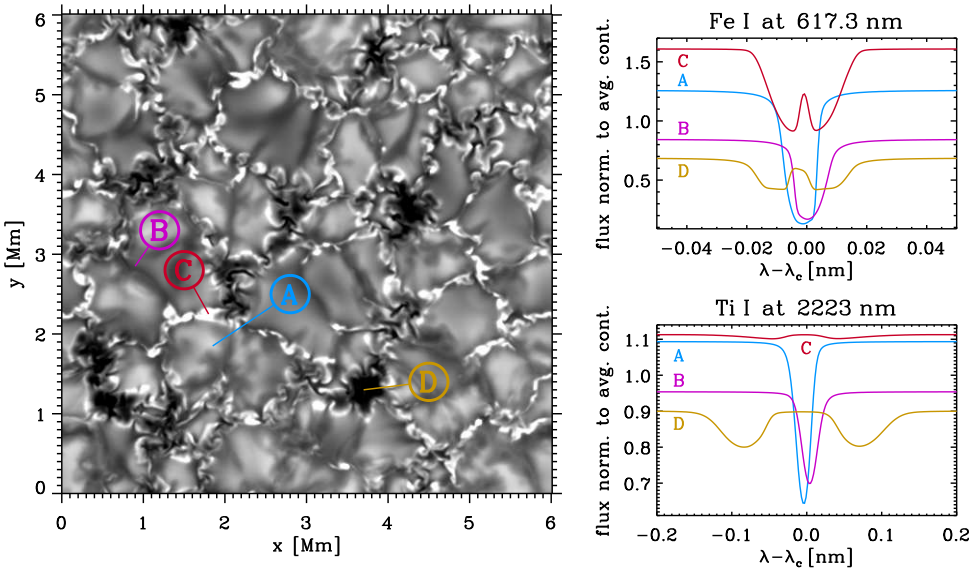

Figure 2.: *Local spectral line profiles. Left panel: Bolometric intensity map of a snapshot from the K0V-star simulation with four points (A to D) marked. Right panels: Local spectral line profiles (normalized to the mean continuum level) at the four points marked in the left panel for two spectral line (top:* Fe I *at 617.3 nm; bottom:* Ti I *at 2223 nm)*

tween M dwarfs and the hotter main-sequence stars. While in the hotter stars the bright magnetic features are very pronounced even at an average field of 500 G, in the M stars there are only very few bright structures and many more dark ones. The depressions in the optical surface of magnetic flux concentraions in these stars are much shallower compared to their horizontal size than on hotter stars. Beeck (2014) shows that these structures are essentially at rest and have an intensity of only 80–90% of the mean intensity while the typical spatial variation of the intensity is only 2–3% in the non-magnetic M star simulations.

3.2 Zeeman effect and thermodynamic effects of the magnetic field

Figure 2 compares the local profiles of two spectral lines (Fe I at 617.3 nm and Ti I at 2223 nm) at four different points (*A* to *D*) for a snapshot of the K0V star simulation with 500 G average field. Two points (*A* and *B*) are weakly magnetized points: *A* is part of an upflow, *B* is situated in a non-magnetic downflow. Consequently, the spectral line is shifted to the blue in *A* and to the red in *B*. The different temperatures at these two points result in different line depths and different continuum levels. The depth dependence of the line-of-sight velocity affects the line profiles in the form of asymmetries (especially for the strongly saturated Fe I line). The other two points are located in magnetic structures: *C* is the center of a small, bright structure, *D* is in the darkest part of an extended dark structure. As both lines have high Landé factors (2.5 and 1.6, respectively), the Zeeman effect splits the line profiles into its Zeeman components. The height-dependent magnetic field is responsible for asymmetries of the individual components. The equivalent width of the Fe I line is similar in *C* and *D*. In a disk-integrated line

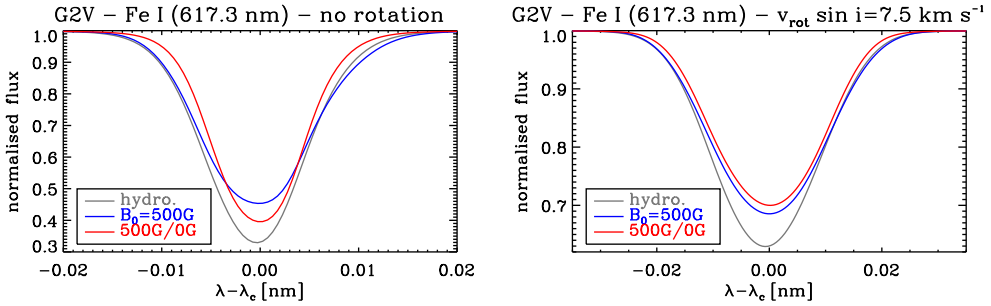

Figure 3.: *Illustration of the relative effects of Zeeman effect and thermodynamic differences between non-magnetic and magnetic simulations (here: G2V) on the* Fe I *line profile. The gray curve corresponds to the average disk-integrated line profile of the non-magnetic simulation, the blue curve corresponds to the average disk-integrated line profile of the run with 500 G average field. The red curve shows the line profile calculated from the same atmosphere as the blue curve, but with the Zeeman effect ignored.*

profile, *D* will, however, have a lower weight than *C* as the integrated (absorbed) flux of the spectral line is lower due to the strong difference in continuum level. The Ti I line is very sensitive to the temperature in the typical temperature regime of the K0V star photosphere (mostly owing to ionization of titanium). This leads to a substantial weakening of the Ti I line in bright (=hot) structures: the equivalent width of the Ti I line at *C* is strongly reduced to only a few percent of its value at the other points. For this spectral line, bright magnetic structures such as at *C* do not contribute much to the disk-integrated line profiles.

As Figure 2 shows, the formation of bright and dark magnetic structures results in very different modifications of the local profiles of the same spectral line in the same atmosphere. Figure 3 shows the disk-integrated profile of the Fe I line at 617.3 nm, without rotation (left panel) and with a solar-like differential rotation with $v_{\rm eq} \sin i = 7.5\,{\rm km\,s^{-1}}$ (right panel). The gray curves are the average line profiles resulting from six snapshots of the non-magnetic (hydrodynamic) run of the G2V star, while the blue curves are the corresponding profiles resulting from six snapshots of the magnetohydrodynamic run of the G2V star with 500 G average field. The red curve results from the same six snapshots (G2V, 500 G), but for the line calculation the field was ignored (i. e. the Zeeman effect was artificially turned off). The difference between the blue and red curves is thus only due to the Zeeman effect, while the thermodynamic local modifications of the atmosphere owing to the magnetic field cause the difference between the gray and the red curve. Without rotation (left panel), the thermodynamic modifications reduce the equivalent width and introduce a relative redshift of the line. The reduced equivalent width results from the existence of bright magnetic structures. At solar photospheric conditions, the Fe I line at 617.3 nm is strongly temperature sensitive and a similar effect of line weakening as for Ti I in the K0V star (see point *C* in Fig. 2) can be observed. The relative redshift can be explained by an increase of the filling factor of downflows and a higher downflow speed at the same optical depth in the magnetic simulation runs (see Beeck, 2014, for more details). The Zeeman effect broadens the line significantly and increases the equivalent

width (owing to reduced saturation). With a rotation rate of $7.5\,\mathrm{km\,s^{-1}}$, which is a typical rotation rate for stars somewhat more active than the Sun, the rotational broadening is, however, already much stronger than the Zeeman broadening and the thermodynamic effects clearly have a bigger impact on the line profile than the Zeeman effect. Magnetic field measurements neglecting the effects of the magnetic field on the convection probably suffer from the impact of the difference in thermodynamic structure between the magnetized and the non-magnetized atmosphere.

4. Conclusion

4.1 Discussion

As illustrated by our 3D simulations, stellar magnetic fields interact with convective flows and locally modify the convection as well as the radiative properties of the stellar photospheres. As a consequence, local concentrations of magnetic field have thermodynamic properties which are very different from the surrounding atmosphere. The resulting spectral line profiles do not only show a Zeeman splitting/broadening but also the signatures of the modified thermodynamics. In some cases, line weakening (due to, e. g., ionization in the bright magnetic structures) can strongly reduce the equivalent width of the lines in concentrations of magnetic field. Beeck (2014) shows that this results in a underestimation of Bf (where B is the field strength of the magnetic part of the star and f is the area fraction covered by B) in a two-component-model fit to the spectral line profiles if one neglects the thermodynamic effects for the fit. In order to accurately measure the magnetic field and other properties of a stellar atmosphere, the active role of the magnetic field must be taken into account.

4.2 Outlook

So far, only unipolar regions of moderate average field strength of up to 500 G have been simulated. The next step will be the simulation of regions with stronger mean magnetic field (starspot umbrae), or more complex geometries (e. g., bipolar regions). For the disk-integrated line profiles we assumed the star to be homogeneous on large scales. We plan to synthesize time-dependent spectra (all four Stokes parameters) of a star with large-scale surface inhomogeneities, such as active regions, star spots etc. Eventually, we aim at a comparison to observational data and the calibration or correction of existing methods to detect and characterize magnetic fields and their global and local organization on cool main-sequence stars.

Acknowledgements. The authors acknowledge research funding by the Deutsche Forschungsgemeinschaft (DFG) under the grant SFB 963/1, project A16.

References

Anders, E. & Grevesse, N. 1989, GeCoA 53, 197

Beeck, B., Collet, R., Steffen, M., Asplund, M., Cameron, R. H., Freytag, B., Hayek, W., Ludwig, H.-G., & Schüssler, M. 2012, A& A 539, A121

Beeck, B., Cameron, R. H., Reiners, A., & Schüssler, M. 2013, A& A 558, A48

Beeck, B., Cameron, R. H., Reiners, A., & Schüssler, M. 2013, A& A 558, A49

Beeck, B. 2014, Diss. Univ. Göttingen,
`http://hdl.handle.net/11858/00-1735-0000-0022-5EC8-D`

Donati, J.-F., Collier Cameron, A., Semel, M., Hussain, G. A. J., Petit, P., Carter, B. D., Marsden, S. C., Mengel, M., López Artiste, A., Jeffers, S. V., & Rees, D. E. 2003, MNRAS 345, 1145

Reiners, A. 2012, LRSP 9, 1

Rempel, M., Schüssler, M., & Knölker, M. 2009, ApJ 691, 640

Rogers, F. J., Swenson, F. J., & Iglesias, C. A. ApJ 456, 902

Rosén, L. & Kochukhov, O. 2012, A& A 548, A8

Vögler, A. 2003, Diss. Univ. Göttingen

Vögler, A., Bruls, J. H. M. J., Schüssler, M. 2004, A& A 421, 741

Vögler, A., Shelyag, S., Schüssler, M., Cattaneo, F., Emonet, T., & Linde, T. 2005, A& A 429, 335